Pergamon

Int. J. Solids Structures Vol. 35, No. 22, pp. 2959–2973, 1998

0020–7683/98 $19.00 + .00

PII: S0020–7683(97)00352–1

EXPERIMENTAL INVESTIGATION OF TRANSIENT THERMOELASTIC EFFECTS IN DYNAMIC FRACTURE

D. RITTEL*
Faculty of Mechanical Engineering, Technion, Israel Institute of Technology, 3200 Haifa, Israel

(*Received* 24 *July* 1997; *in revised form* 4 *November* 1997)

Abstract—Thermoelastic effects in fracture are generally considered to be negligible at the benefit of the conversion of plastic work into heat. For the case of dynamic crack initiation, the experimental and theoretical emphasis has been put on the temperature rise associated with crack-tip plasticity.

Nevertheless, earlier experimental work with polymers has shown that thermoelastic cooling precedes the temperature rise at the tip of a propagating crack (Fuller *et al.*, 1975). Transient thermoelastic effects at the tip of a dynamically loaded crack have been theoretically assessed and shown to be significant when thermal conductivity is initially neglected (Rittel, 1997). However, the fundamental question of the relation between crack initiation and thermal fields, both of transient nature, is still open.

In this paper, we present an experimental investigation of the thermoelastic effect at the tip of fatigue cracks subjected to mixed-mode (dominant mode I) dynamic loading. The material is commercial polymethylmethacrylate as an example of "brittle" material.

The applied loads, crack-tip temperatures and fracture time are *simultaneously* monitored to provide a more complete image of dynamic crack initiation. The corresponding evolution of the stress intensity factors is calculated by a hybrid-experimental numerical model.

The results show that substantial crack-tip cooling develops initially to an extent which corroborates theoretical estimates. This effect is followed by a temperature rise.

Fracture is shown to initiate during the early cooling phase, thus emphasizing the relevance of the phenomenon to dynamic crack initiation in this material as probably in other materials. © 1998 Elsevier Science Ltd. All rights reserved.

1. INTRODUCTION

Many years ago, Taylor and Quinney (1934) showed that the major part of the plastic strain energy invested in deforming a metal is converted into heat. Since the mechanical properties of materials are affected by temperature, a natural trend in research has been to consider cases in which the strain energy is converted into heat.

Consequently, investigations of dynamic crack initiation and/or propagation stages have essentially addressed the *temperature rise* at the crack-tip as a result of extensive plastic deformation. For example, recent work on dynamic impact fracture shows that very large temperatures can develop at the crack-tip, thus accelerating the failure process, either by direct fracture or by shear band formation (see, e.g. Zhender and Rosakis, 1991; Zhou *et al.*, 1996).

In this work and many others, the general trend is to neglect crack-tip thermoelastic effects at the benefit of the thermoplastic behavior of the material.

Let us now refer specifically to the experimental work of Fuller *et al.* (1975) and to the numerical-experimental investigation of Weichert and Schönert (1978). Both works address *temperature rise* or *heat generation* at the tip of the propagating crack. It is thus quite interesting to note that noticeable *thermoelastic cooling* effects are shown (and briefly addressed) in Fuller *et al.* (1975) who investigated propagating cracks in polymers. Weichert and Schönert (1978) investigated the temperature rise during fracture of glass plates. Their

*Fax: (972) 4 832 45 33. E-mail:rittel@dany.technion.ac.il.

results clearly show that fracture initiates during the initial cooling phase followed by a later temperature increase. This point is not addressed.

Therefore, these result show that when short time scales characteristic of dynamic crack-initiation and/or rapid propagation are involved, noticeable transient thermoelastic effects are observed.

However, in the above-mentioned experimental work, the accurate fracture time was not recorded and quoted as these studies addressed propagating cracks.

Without this capital information, the question remains as to when did fracture actually initiate with respect to the thermal events sequence.

The tip of a crack is a very special locus where large tensile triaxial stresses develop. Rittel (1997) showed that under transient conditions—where heat conduction is neglected and adiabatic conditions prevail—the solution of the heat equation for a thermoelastic solid predicts significant crack-tip cooling.

In this paper, we will pursue this line of investigation by bringing new experimental evidence about crack-tip thermoelastic effects under transient loading. Specifically, we *simultaneously* monitor the applied loads, crack-tip temperature and fracture time.

As a result, it will be shown that for an elastic material, the thermoelastic temperature drop is significant and deserves additional consideration with respect to dynamic failure criteria.

The paper is organized as follows: in the second section we briefly review the essential theoretical results and assumptions related to the transient thermoelastic effect. Next, we describe and discuss the experimental setup used to investigate this effect. We then present and discuss the experimental results obtained. The last section summarizes and concludes this work.

2. THEORETICAL BACKGROUND

The heat equation is given by (Boley and Weiner, 1960):

$$k\nabla^2 T-\alpha(3\lambda+2\mu)T_0\dot{\varepsilon}^e_{kk}+\beta\sigma_{ij}\dot{\varepsilon}^p_{ij}=\rho c\dot{T} \tag{1}$$

where k is the heat conductance and α is the thermal expansion coefficient. ρ, c, λ and μ stand for the material's density, heat capacity and Lamé constants, respectively. T is the temperature and the strain rates $\dot{\varepsilon}$ are divided into elastic and plastic. Finally the factor β expresses the fraction of plastic work converted into heat (typically 0.6 for polymers and 0.9 for metals).

Consider now a thermoelastic cracked solid. If adiabatic conditions prevail during the first instants of the transient loading ($k\nabla^2 T=0$), eqn (1) shows that the rate of change of the temperature is related to the rate of change of the hydrostatic pressure p (α, ρ and c being the linear expression coefficient, density and heat capacity coefficient, respectively).

$$T(t)=T_0\left(1+\frac{3\alpha}{\rho c}\rho(t)\right) \tag{2}$$

The crack-tip stresses are described using linear elastic fracture mechanics (LEFM) concepts, mostly the stress intensity factors (K). For a crack subjected to arbitrary loading, the contribution of each mode to the overall hydrostatic pressure can be added separately. As an example, consider a point located in the K dominated zone (valid LEFM assumptions) along the crack-line ($\theta=0$) at a distance r from the tip. For the *stationary* crack subjected to mode I transient loading under plane strain, eqn (2) becomes the simple following expression (Rittel, 1997):

$$T(t) = T_0\left(1 - \frac{2\alpha(1+\nu)}{\rho c}\frac{K_I(t)}{\sqrt{2\pi r}}\right) \tag{3}$$

The influence of the transient loading appears through the time dependence of the stress intensity factor—$K(t)$—whose determination has been studied e.g. by Bui *et al.* (1992) and by Maigre and Rittel (1993), among others. The interesting point about eqn (3) is that it predicts crack-tip cooling (as long as the material remains elastic) with the $r^{-1/2}$ singularity from LEFM.

This singularity causes the same paradox as in LEFM about infinite crack-tip stresses, that is infinite cooling, which can be lifted by allowing yielding of the material.

Therefore, by analogy with the coexistence of a plastic zone surrounded by an elastic one, the present approach predicts the development of a hot enclave (plastic) surrounded—and thermally isolated from—a cold zone (elastic). At this point, let us note that the plastic zone is always smaller than the elastic and that its size is variable, in inverse proportion to the square value of the yield strength of the material.

3. EXPERIMENTAL

3.1. *Foreword*

In the experiments to be described below, our goal is to measure simultaneously the applied loads, crack-tip temperature and fracture time. Each point will be discussed separately.

3.2. *Experimental setup*

The experimental apparatus will be briefly described as it has been described in detail previously (Rittel *et al.*, 1992). As shown in Fig. 1, the specimen, called the compact compression specimen (CCS), is designed such as to cause crack opening under compressive loads. The specimen is brought into contact with an instrumented (strain gage) bar against which a striker can be fired at velocities ranging from 8–65 m/s. When the striker hits the bar, a compressive stress wave progresses towards the specimen, being partly transmitted-partly reflected at the specimen-bar interface. These signals, which are collected on the strain gage of the bar are shifted in time (space) and corrected for geometric dispersion (Lifshitz and Leber, 1994), to coincide with the specimen-bar interface. The shifted incident

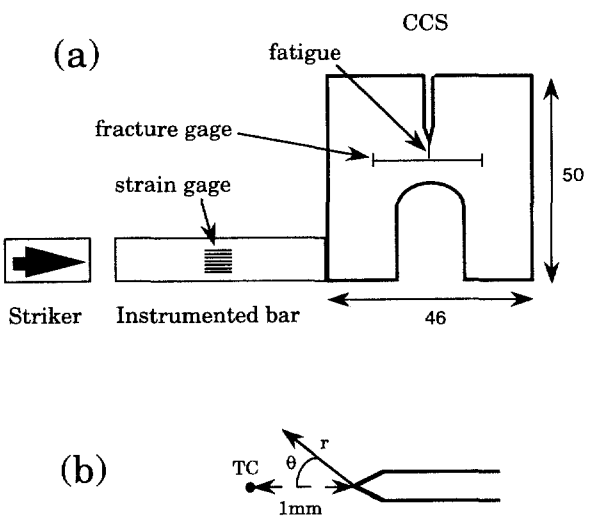

Fig. 1. The experimental setup. The compact compression specimen is brought in contact with an instrumented bar. The specimen is instrumented with a fracture gage and an embedded thermocouple (TC). The applied loads, fracture time and crack-tip temperatures are monitored simultaneously (all dimensions in mm).

Table 1. Measured mechanical properties of the commercial PMMA used in this study (Rittel and Maigre, 1996)

	Young's modulus [GPa]	Poisson's ratio
Static	3.70	0.42
Dynamic	5.76	0.42

and reflected signals are thus used to determine the boundary conditions (force and/or velocity) prescribed to the specimen (Rittel *et al.*, 1992). Throughout the experiment, the CCS is unsupported and it separates from the bar a short while after impact. Fracture is purely inertial as a result of the stress waves in the specimen.

3.3. *Experimental material*

We chose to work with commercial polymethylmethacrylate (PMMA), as a model "brittle" material. The dynamic fracture properties of this material have been characterized by Rittel and Maigre (1996), who observed a marked dependence of the dynamic fracture toughness on the loading rate (impact velocity). The mechanical properties of our PMMA were previously determined, as summarized in Table 1.

3.4. *The specimen and its instrumentation*

A fatigue precrack was carefully grown from the notch of each CCS to achieve crack-tip sharpness. The specimen thickness was 12.5 mm.

On one side, a single wire fracture gage was painted using conductive silver paint. In all the specimens, the fracture gage was located 1 mm ahead of the fatigue crack-tip. The typical thickness of the painted wire varied from 200–300 microns.

On the other side of the specimen, opposite to the fracture gage, a small hole (0.3 mm diameter) was drilled to a typical depth of 6 mm to allow embedding of the active junction of a *K*-type (Chromel–Alumel) thermocouple. The wire thickness was 120 microns and the typical sensing bead radius was 130 microns. The bead was sealed using acrylic cold mounting polymer (Technovit, Kulzer) whose thermal properties are assumed to be close to those of the investigated PMMA. The other junction of the thermocouple was embedded in the arm of the specimen which was not directly impacted. This junction was used for compensation of global effects due to the stress waves in the specimen. The signals from the two junctions were differentially fed into a 12 bit/10 MHz Nicollet 490 oscilloscope. Two additional channels of the oscilloscope were used to record the fracture gage and the strain gage signals.

A total of 12 specimens served for the basis of this study while many more specimens were tested, including different materials whose results will be reported in the future.

3.5. *Preliminary thermal experiments*

The goal of the following experiments was to evaluate the applicability of the embedded thermocouple technique to transient temperature measurements. A series of experiments were carried out on 10 mm diameter and 4.5 mm thickness disks made of commercial polycarbonate (PC) and polymethylmethacrylate (PMMA). Here too, a hole was drilled at mid-thickness of the disk to allow embedding of the sensing tip of a *T*-type (copper–constantan) thermocouple was identical in its dimensions to the *K*-type thermocouple.

The experiment consisted of inserting the disk between two instrumented bars (Kolsky-bars). We only recorded the incident bar signal and the thermal signal to provide a qualitative assessment of the thermocouple's response. A total of 12 such disks were tested.

4. RESULTS

4.1. *Transient response of the embedded thermocouple*

Figure 2 shows typical results for the above mentioned experiments. The incident stress waves reaches the specimen 72 microseconds after being recorded at the strain gage on the

incident bar. The signal reflected at the specimen-bar interface is thus detected after 144 microseconds. Until impact, the thermal signal remains constant and very soon after the thermal signal is recorded. For the more "ductile" PC specimens, the specimen remains in place between the bars and is repeatedly impacted by the stress waves travelling back and forth in the bars. As can be seen in Fig. 2(a), the temperature rises stepwise according to the repeated impact. In Fig. 2(b) a selected part of the thermal signal has been blown up

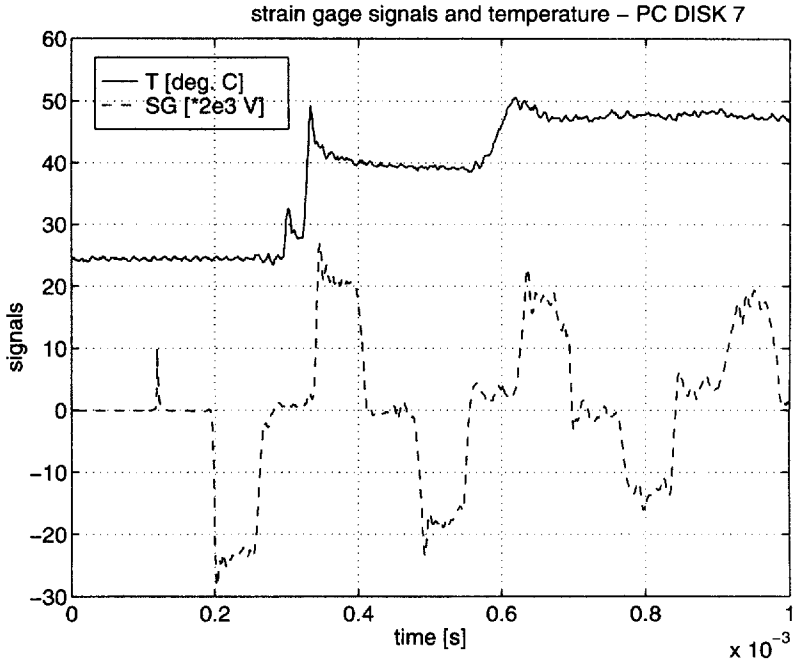

Fig. 2(a). Experimental signals recorded during impact of a polycarbonate disk. The dashed line shows the stress wave travelling back and forth in the bar, thus repeatedly hammering the disk. The thermal signal (solid line) increases stepwise as a result of the accumulated plastic deformation.

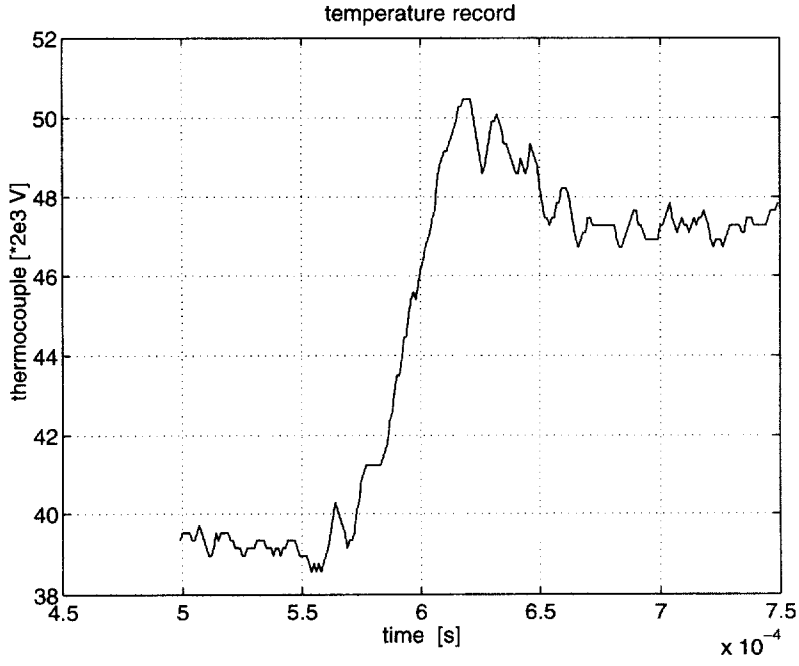

Fig. 2(b). Blown up section of the thermal signal. Note the very short rise time of less than 10 μs.

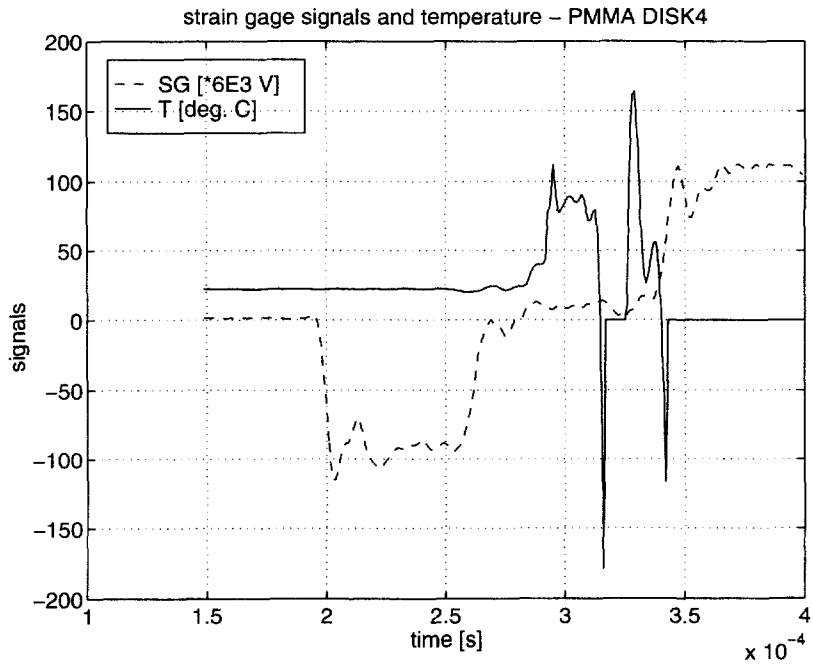

Fig. 2(c). similar to (a) with more "brittle" PMMA disk. Fracture occurs very soon after the initial temperature rise and the thermal signal starts to oscillate violently.

and it can be noted that the rise time of the thermal signal is very short, typically of the order of 10 microseconds. For the more "brittle" PMMA disks, the specimen shatters soon after impact. The temperature increases very rapidly and the signal becomes highly disordered thereafter (Fig. 2(c)).

The temperature rise can be attributed to the plastic deformation and fracture of the specimen while the disordered part of the signal comes from the deterioration of the thermocouple itself due to specimen fracture.

These experiments show that the embedded thermocouple has a very short response time of the order of 10 microseconds. As such, this technique is suitable for transient crack-tip thermocouple measurements as discussed next.

4.2. *Dynamic fracture of compact compression specimens*

Figure 3(a) shows typical recordings from one point impact experiments. Here again, the stress wave reaches the specimen typically 72 microseconds from the onset of the incident compressive pulse. Until this time, no thermal signal is recorded. 10–25 microseconds after the stress wave has reached the interface, some weak variations of the thermal signal are noticeable followed by an abrupt drop and then by a steep increase. The fracture gage (mid-span, 250 microseconds) is used to trigger the overall recordings. Past fracture the signal oscillates violently.

Fracture, as detected by the wire gage, occurs almost always during the ascending phase of the thermocouple, as shown in the magnified Fig. 3(b).

The extent of the temperature drop and its ratio with respect to the temperature rise varied from specimen to specimen but the effect was identical in all specimens: noticeable temperature drop followed by a temperature rise during which the wire gage indicated fracture.

Two distinct fracture paths were observed: the first path crossed the thermocouple containing hole, corresponding to a small kink angle value. In this case the thermocouple was directly damaged in most occasions. The second fracture path avoided the thermocouple. The crack bifurcated before reaching the thermocouple which was left in the specimen at a variable distance (of the order of 1 mm) beneath the fracture path. These

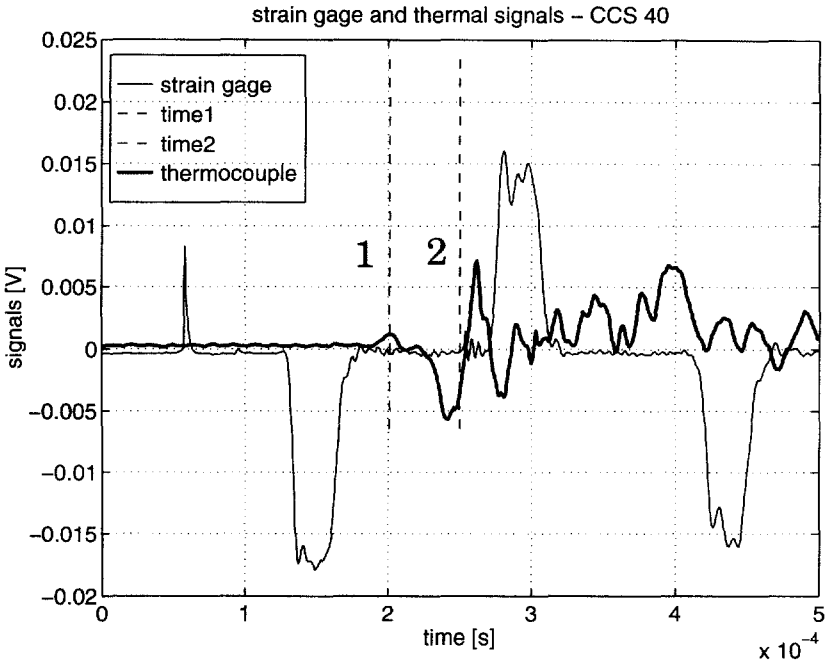

Fig. 3(a). Experimental signals recorded during impact of CCS40. The stress wave reaches the specimen at time 1 = 72 μs. About 15 μs later the thermal signal drops during 25 μs. It then raises in a very short period of time during which fracture is recorded at time 2 = 250 μs.

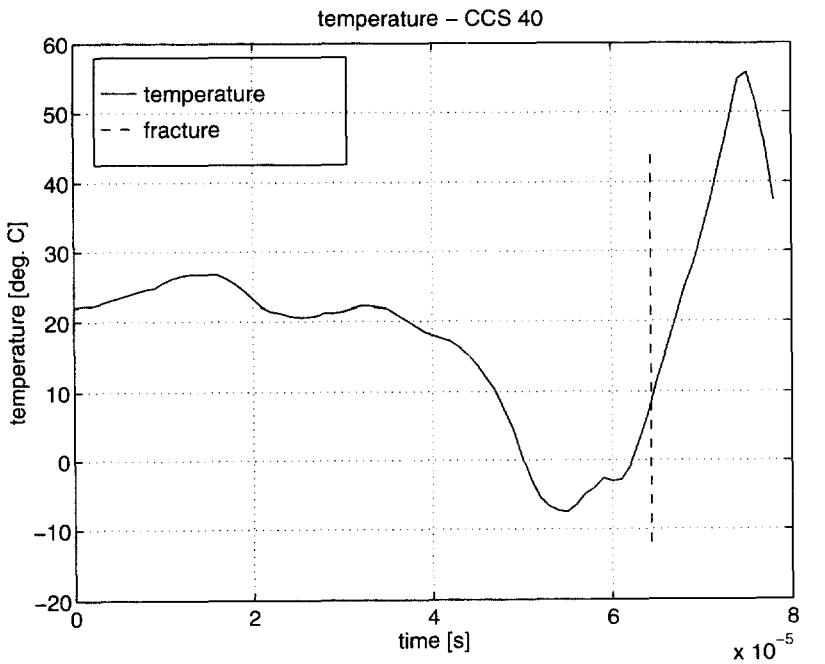

Fig. 3(b). Blown up part of Fig. 3(a) showing the temperature recorded in the vicinity of fracture time.

paths and their combinations (two cracks) are shown schematically in Fig. 4. The details of the temperature record depend on the details of the crack path and the proximity of the crack-tip to the sensing bead. Its general characteristics (cooling and heating sequence) are similar for all the specimens, as previously mentioned.

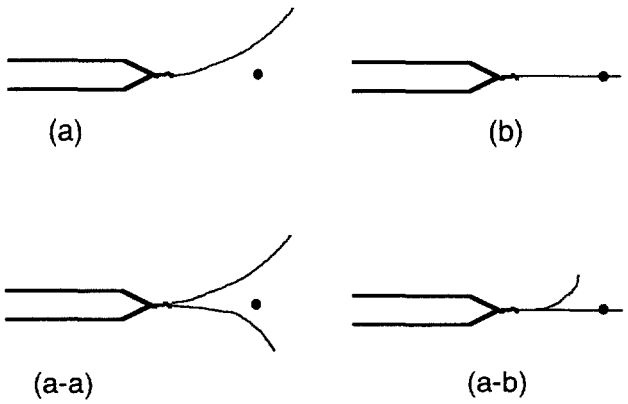

Fig. 4. The various crack paths observed and their relationship with the thermocouple marked by the black dot.

Table 2. Experimental parameters: the impact velocity, the minimum temperature recorded prior to fracture (T_{min}) and the corresponding time (t at T_{min}). Fracture time (from the fracture gage) is indicated by t_f. The crack path is indicated by a for kinked crack and b for a straight crack or their combination, as shown in Fig. 4

CCS	v impact [m/s]	T_{min} [°C]	t at T_{min} [μs]	fr. time (t_f) [μs]	T at t_f [°C]	t_f-$t_{T_{min}}$ [μs]	path
31	27	−16.0	50.0	60.0	40	10.0	a–b
34	22	9.1	63.5	76.5	39	13.0	a–a
35	15	−62.0	45.9	77.5	64	31.6	b
36	12	18.8	39.2	75.3	34	42.4	b
37	16	0.0	52.8	83.3	78	30.5	a
38	8	16.3	61.0	95.0	−11	34.0	b
39	34	11.5	217.0	250.0	46	33.0	a–a
40	29	−7.6	55.3	64.3	6	9.0	a–a
41	30	−61.0	78.2	75.2	−50	−3.0	a–b
42	32	−41.0	67.0	74.5	52	7.5	a–b
43	23	−3.0	40.5	73.5	65	33.0	a
44	28	−18.0	242.0	250.0	−3	8.0	a–b

In Table 2 we have summarized various relevant parameters such as the recorded minimal temperature, temperature at fracture time, fracture time, fracture path, and impact velocity.

5. DISCUSSION

5.1. *The embedded thermocouple technique (ETC)*

Transient temperature measurement is generally carried out using non-contact techniques (IR detectors, Zhender and Rosakis, 1991) or thermocouples cemented to the surface of the specimen. Thin sensing junctions have been especially devised to achieve a fast response (Bendersky, 1953).

To work with polymers, we use small size embedded thermocouples. There is no straightforward way to calibrate the embedded thermocouple, by opposition with a bare one which can be exposed to e.g. short laser pulses or a hot fluid. One practical way to generate transient temperatures rises is to take advantage of the conversion of plastic work into heat as mentioned in the introduction. This was the reason underlying our experiments with small polymeric disks. Our experiments show that the embedded thermocouple technique provides a simple means to measure transient temperatures with a very short rise time. The technique thus proved to be suitable for the projected dynamic fracture experiments.

Additional insight into the transient response of such a thermocouple is gained by considering the sensing bead as a sphere of radius a to which constant surface temperature

T_0 is prescribed. The average temperature of the sphere is given by (Carslaw and Jaeger, 1959):

$$T_{av}(t) = T_0 - \frac{6T_0}{\pi^2} \sum_{n=1}^{\infty} \frac{1}{n^2} e^{-\kappa n^2 \pi^2 t/a^2} \tag{4}$$

Figure 5 represents the response of a 130 micron radius sphere with a thermal conductivity κ of 10^{-5} m^2/s, as typical of most metals. From this figure, it can be seen that a significant (average) response can be obtained in very short times of the order of 15 microseconds. The exact temperature distribution is given by:

$$T(r, t) = T_0 + \frac{2aT_0}{\pi r} \sum_{n=1}^{\infty} \frac{(-1)^n}{n} \sin \frac{n\pi r}{a} e^{-\kappa n^2 \pi^2 t/a^2} \tag{5}$$

The time derivative of eqn (5) describes the unit impulse response of the thermocouple. In this case, a physical choice must be made as to the effective depth at which this response is to be calculated. In Fig. 6 we have plotted the unit impulse response for the above mentioned thermocouple where the "control" depth was chosen to be 5% of the radius beneath the surface. This choice is of course arbitrary as we have no *a priori* knowledge of an effective depth required to generate the thermoelectric effect. This response can be used to deconvolve the experimentally recorded signals from the thermocouple.

Figure 7 shows the original and deconvolved signals. The deconvolution procedure adds some noise to the signal. Yet it can be noted that the actual (deconvolved) signal occurs slightly earlier and with higher values than the measured one. However, as mentioned in the preceding discussion, the response function depends on some adjustable parameters so that we will not address further this point. We will use the [actual] measured signals assuming that the actual signals are probably not very different.

As to the ETC technique itself, it must be noted that it is seldom used. Chou *et al.* (1973) embedded thermocouples in polymers when they investigated thermomechanical aspects of the deformation of these materials as a function of the strain rate. Their thermal measurements were carried up to a maximum strain rate of 45 s^{-1}. At higher strain rates

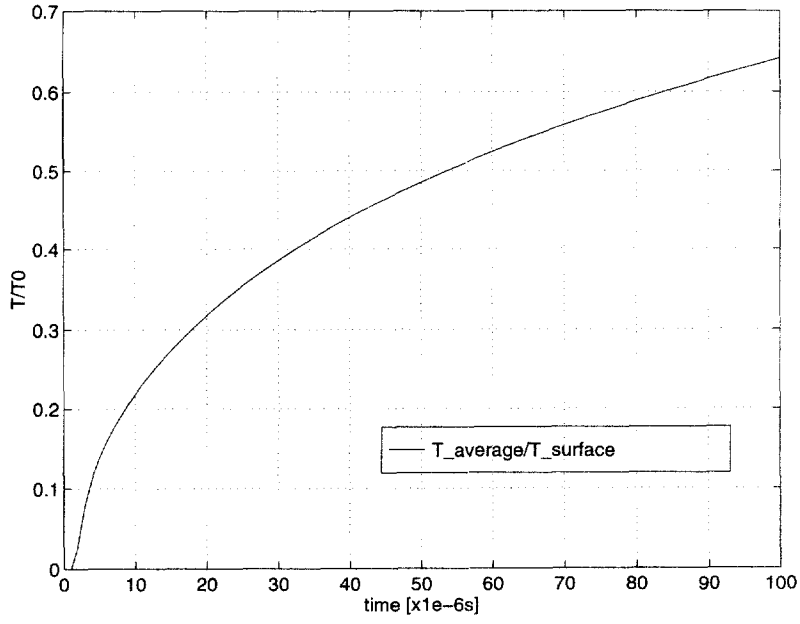

Fig. 5. Average temperature in a sphere representative of the thermocouple's sensing tip. Prescribed surface temperature T_0.

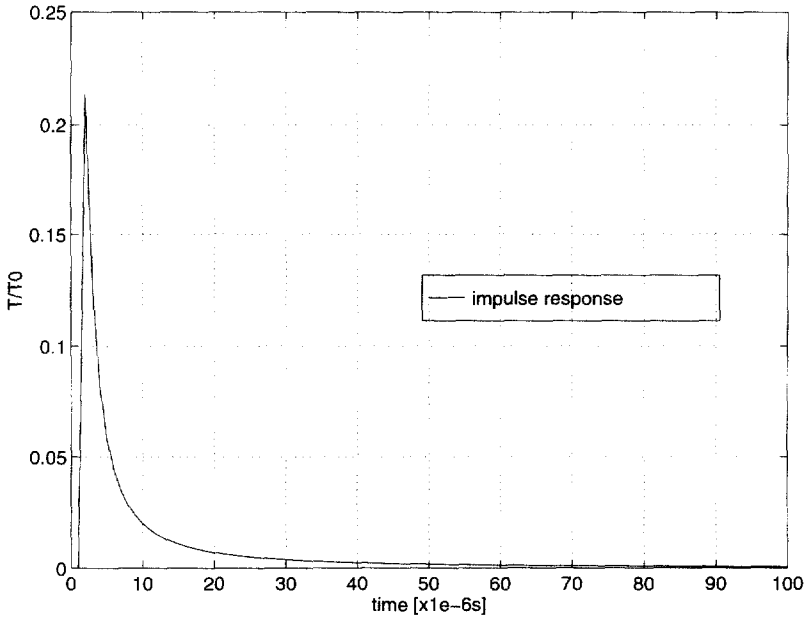

Fig. 6. Impulse response of the sphere analyzed in Fig. 5. The depth at which the temperature is analyzed equals 0.05 times the spheres radius (130 μ).

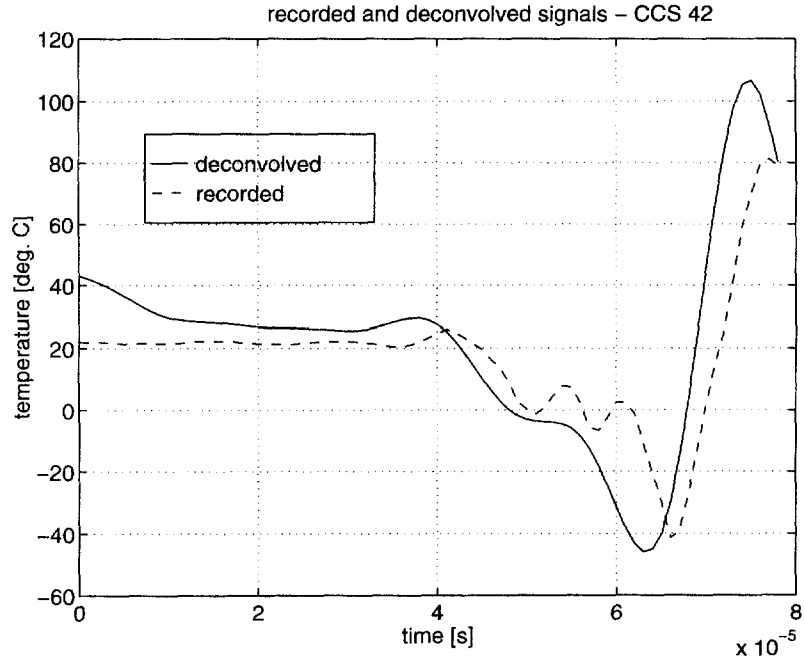

Fig. 7. Recorded and deconvolved thermal signals for CCS 42 in the vicinity of fracture time. Deconvolution was carried out *w/r* to the response characteristics shown in Fig. 6. Note that the deconvolved signal occurs earlier and at slightly higher amplitudes than the measured one.

(760 s^{-1}), these authors calculated a temperature rise of the order of 15°C. Our experiments dictate a strain rate of about 3×10^3 s^{-1} and we measure comparable temperature rises. Consequently, the embedded thermocouple technique is a valuable tool for the investigation of dynamic fracture of polymers.

5.2. *The temperature records during dynamic fracture*

As shown in Table 2, the range of impact velocities was 8–34 m/s. At the lower impact velocities, the crack-path goes straight through the thermocouple whereas at higher velocities, additional kinked cracks are observed. In all cases, one of the cracks goes through or close enough to the thermocouple to yield a valid thermal recording. However, the variety of observed fracture paths makes a quantitative comparison difficult at this stage. A similar difficulty was noted by Döll (1976) who investigated dynamic crack propagation in polymers. Despite this discrepancy in fracture paths, our experimental results are very similar to those reported by Fuller *et al.* (1975) in the sense that they show a *definite amount of crack-tip cooling prior to the heating phase*. It must be noted that these authors used a non contact technique as opposed to the thermocouples of this study. The overall time necessary for the temperature to rise from its minimal value to its value at observed fracture reached an extreme value of 40 microseconds but was usually smaller.

Two important points will be now addressed : the "timing" of the fracture with respect to the thermal events and the physics of the cooling itself, as observed in our setup.

5.3. *The "timing" of fracture*

Our results show that fracture is always detected in the transition between cooling and rapid heating as sensed by the thermocouple. This result is identical to the observations of Fuller *et al.* (1975) who reported a noticeable temperature rise when the crack-tip was sensed by the infrared detector. In our experiments, the fracture sensor is located 1 mm ahead of the crack-tip. A first estimate of fracture time must therefore be shifted by a time equal to this distance divided by the crack velocity. While we did not measure the actual crack velocity, a reasonable value would lie between 100–300 m/s for such experiments (Rittel and Maigre, 1996). A first estimate of fracture time would thus require a shift of 3–10 microseconds prior to the fracture gage reading.

Accurate determination of the fracture time is a capital problem in such experiments which amounts in fact to the very definition of fracture. Aoki and Kimura (1993) investigated the effects of internal crack formation on a surface detection mechanism (caustics). Their result is that the surface detection of the fracture process lags behind the actual fracture. This problem was also addressed by Maigre and Rittel (1996) who used the dual (reciprocal) formulation of the H-integral (Bui *et al.*, 1992) to determine a "bulk" fracture time on the basis of measured interfacial velocities and forces. Their results showed that there is a delay of about 10 microseconds between the "bulk" fracture time and the fracture times, as measured by a surface timing wire. Such delay could be tentatively identified at the postulated "incubation" time (Kalthoff and Shockey, 1977).

Consequently, these two added delays indicate that the fracture process started most likely 13–20 microseconds prior to the fracture gage recording.

By contrast, the thermal signal reading can be considered as "instantaneous" as it is related to the crack-tip elastic straining.

This is an indication that fracture initiated on the average during the cooling phase.

This result is new and was not reported earlier to the best of our knowledge. Whereas it cannot be extended at present in a straightforward manner to other materials, it nevertheless bears an important information about dynamic crack initiation, namely that thermoelastic effects should not be overlooked. Therefore, the *entire thermal sequence* (both the cooling and heating stages) are relevant to dynamic crack initiation, and most likely propagation too. This sequence is complemented by measuring (or estimating as in Weichert and Schönert, 1978) the fracture time.

5.4. *The physics of the thermoelastic cooling*

The physics underlying the observed cooling lies in the dominance of thermoelastic effect while neglecting heat conduction away from the fracture zone. Such assumption is customarily done when seeking an estimate for the maximum temperature by converting plastic work into heat. This point is also supported experimentally by Zhender and Rosakis (1991). We make the same assumption to interpret our physical observations.

For a stationary crack subjected to mixed-mode loading, the expected temperature distribution—$T(r, \theta)$—can be assessed from the knowledge of the stress intensity factors $K_I(t)$ and $K_{II}(t)$. To do so, we use eqn (2) into which the general form of the crack-tip stress fields for mixed-mode loading has been substituted. As an example, eqn (3) was earlier derived as the special case of mode I loading for a distance r and angle $\theta = \theta$. It can be remarked that the cooling effect is maximal at that point and that for the present mixed-mode experiments, the mode II component does not contribute to the process at the selected thermocouple's location.

The stress intensity factors are calculated from a numerical simulation of the experiment (ANSYS, 1994) using the interfacial recorded force pulse as the boundary condition. The specimen is initially at rest and stress free. Such numerical simulations have been carried out in earlier work (e.g. Rittel *et al.*, 1997) and will not be discussed here for the sake of brevity. Let us just mention that we use a boundary condition based on the measured force (rather than displacement) since the specimen-bar separation can be easily modeled by prescribing traction-free conditions for any duration of time. In Fig. 8(a) we show the results of our simulation of one experiment. The stress intensity factors are calculated for the stationary crack and do not include fracture itself. The calculation is valid until fracture time as measured from the fracture gage.

The temperature drop can be assessed as follows. First, the plastic zone radius ahead of the crack ($\theta = 0°$) is calculated according to:

$$r_p = \frac{K_I^2}{2\pi}\left(\frac{1-2\nu}{\sigma_y}\right)^2 \tag{6}$$

The following representative values can be assumed: $\nu = 0.37$, the dynamic (rate sensitive) yield strength of PMMA $\sigma_{yd} = 200$ MPa. For an applied stress intensity factor $K_I = 3$ MPa.m$^{1/2}$, eqn (6) yields a plastic radius $r_p = 2.5 \times 10^{-6}$ m. Next the temperature drop is calculated at a distance $x \geqslant r_p$ using eqn (3). Typical values of $\alpha = 10^{-4}/°K$ and $\rho c = 10^6$ J/m^3/°K are then used in eqn (3) to yield a relative temperature change of $\Delta T/T_0 = 0.146$ at $x = 2r_p$. This amounts to a temperature drop from 20°C (RT) to about −23°C. The

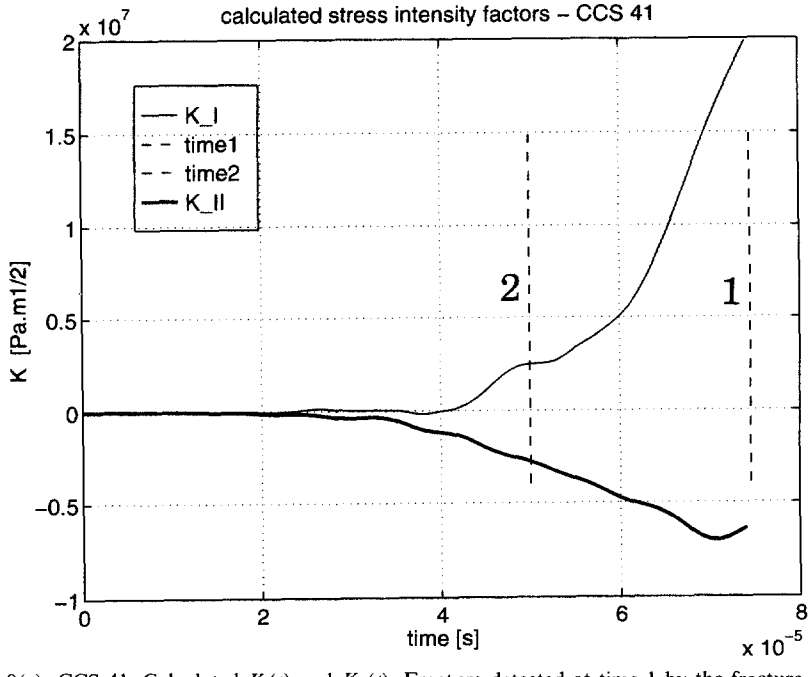

Fig. 8(a). CCS 41. Calculated $K_I(t)$ and $K_{II}(t)$. Fracture detected at time 1 by the fracture gage. Time 2 is the assumed value of the onset of crack propagation for subsequent calculations.

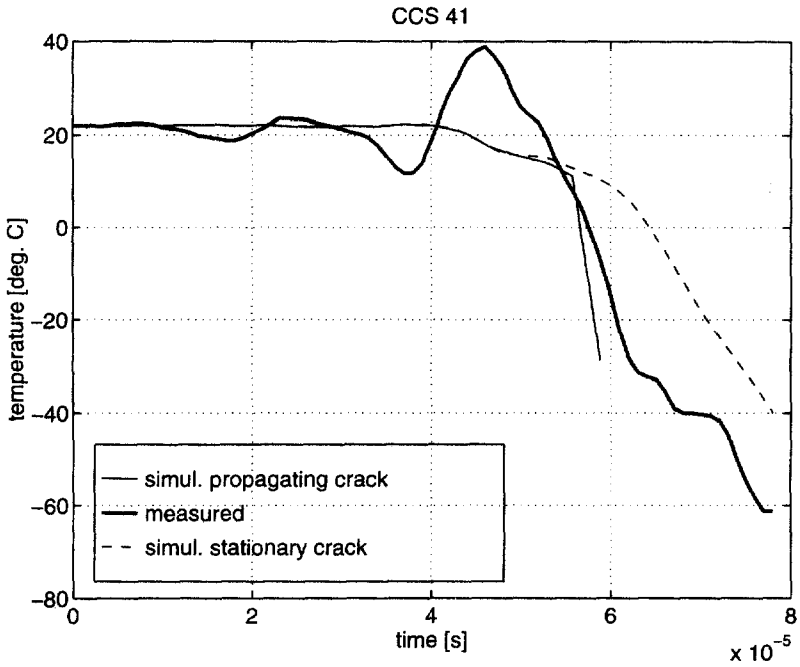

Fig. 8(b). Temperatures. Bold line is the measured temperature. The dashed line shows the calculated temperature using eqn (3) for the stationary crack ($r = 1$ mm). The thin solid line is identical to the dashed one until time 2 from which the crack propagates at constant K_I (time 2) and K_{II} (time 2). The crack velocity is constant (200 m/s). Note that the thin line replicates more closely the measured temperature.

same calculation predicts that the temperature will only drop to 17°C at a distance $x = 400$ r_p (1×10^{-3} m) ahead of the crack-tip.

The above results show that a minimum temperature of the order of −40°C cannot be sensed at a distance of 1 mm from the stationary crack-tip at fracture time. Indeed, this would require an unphysically high value of the stress intensity factor.

This apparent contradiction can be lifted if it is realized that the crack does not remain stationary with respect to the thermocouple. In fact, the crack-tip propagates toward the sensing tip. Therefore, the thermal information comprises the overall crack-tip history from the onset of loading until it starts propagating to pass through (or near) the thermocouple. This point was noted by Fuller *et al.* (1975) who mentioned the thermoelastic cooling precursor signal. However, these authors investigated propagating cracks while this work is concerned with the onset of crack propagation itself.

Given the evolution of the stress intensity factors, the temperature recorded at a fixed location can be estimated using the following simplifying assumptions:

—A decision can be made as to the actual fracture time (t_{af}) w/r to the measured one (t_f) as discussed previously (i.e. assume that $t_{af} = t_f - x$).
—An additional assumption is that the crack starts and continues to propagate at the constant values of $K_I(t_{af})$ and $K_{II}(t_{af})$.
—The last assumption is that of a constant velocity of crack-propagation in range of 100–300 m/s as in Rittel and Maigre (1996).

Of these assumptions, the most restrictive is the second one, as it has been established that the actual crack-tip stress field ahead of a propagating crack cannot be reduced to the singular term (Freund and Rosakis, 1992). However, the goal of our simulation is not to reproduce accurately the actual temperature distribution, but to get a simple idea of the correction induced by the crack motion.

An example of such simulations is shown in Fig. 8(b). The stress intensity factors shown in Fig. 8(a) are used to calculate the thermal signal detected 1 mm ahead of the

stationary crack-tip. The calculation is carried out until fracture time $t_f = 75.2$ μs. Note that at this time, the SIF values are unrealistically high for a polymer. Assuming a more realistic fracture time of $t_{af} = 50$ μs and a propagation velocity of 200 m/s the thermocouple corresponding to the propagating crack can now be calculated. The results show that the calculated thermocouple is much closer to the measured one than when calculated for a stationary crack.

It must be noted that the embedded thermocouple is not modeled in the numerical model of the experiment to keep it as simple as possible. Consequently, the quoted values of the stress intensity factors must be considered as indicative only of the actual values. One important point in such simulation is that, regardless of the actual modeling assumptions, the calculation remains valid for distances between the crack-tip and the thermocouple which are greater or equal to the size of the plastic zone in which the material is assumed to heat up. As shown in Fig. 8(b), when the crack-tip gets closer to the thermocouple, lower temperatures are predicted whose orders of magnitude are similar to the ones measured.

The simulation illustrates the point that the lowest sensed temperature prior to fracture is the situation corresponding to the thermocouple being ideally located at the elastic–plastic boundary, where the cooling effect is the greatest. Such a "stationary" measurement is obviously not practical using thermocouples. Consequently, the evolution of the temperature sensed by the thermocouple is related to the series of crack-tip positions. This includes the extreme condition where the boundary of the plastic zone reaches the thermocouple (the coldest point) immediately followed by the hot plastic zone itself.

The simulation thus combines an estimate of the real fracture time with the corresponding, yet delayed, original thermal information as the crack-tip reaches the sensor at a later time.

Finally, as the crack progresses beyond the sensing tip, two elements contribute to the observed temperature rise: the hot plastic zone and the new surfaces created as the crack intersects the vicinity of the thermocouple (as also noted by Fuller *et al.* (1975)).

The results shown in the this paper indicate the transient crack-tip temperature can be accurately sensed using the embedded thermocouple technique. Specifically, the transient thermoelastic crack-tip cooling is substantial in the investigated polymer in accordance with the theoretical predictions of eqn (4). Fracture is detected during the cooling phase and it is interesting to relate this observation with the temperature dependence of the investigated material's toughness.

The present work shows that thermoelastic effects are not negligible for dynamic fracture of materials with a dominant elastic response. The latter is influenced by the loading rate, and for many materials, the yield strength increases with the rate of loading (Meyers, 1994). Consequently, thermoelastic effects are likely to be more predominant at high loading rates, as observed in this work. It is thus felt that the competition between thermoelastic cooling and subsequent heating should dictate the dynamic fracture properties of a given material.

Finally, since the temperature drop near the crack-tip is significant, it may be interesting to investigate the relevance of the present observations to the well known ductile to brittle transition.

6. CONCLUSIONS

The transient temperature changes at the tip of a dynamically loaded crack have been investigated in commercial PMMA.

- The measurements show that thermoelastic effects are appreciable in the sense that crack-tip temperatures can drop by several tens of degrees. Thermoelastic cooling is followed by a temperature rise due to the plastic zone and/or fracture process itself which exposes new surfaces.
- These results are in accordance with an estimation of the amplitude of thermoelastic cooling under transient conditions, neglecting heat conduction.

- The temperature drop recorded ahead of the crack-tip can be simulated using simplifying assumptions.
- The timing of fracture (onset of crack propagation) is detected during the cooling phase showing the importance of the phenomenon in the investigated material.
- The present results show the relevance of thermoelastic effects in dynamic crack initiation.

Acknowledgements—This research is supported by the Israel Science Foundation under grant no. 030-039 and by Technion VPR Research Fund. Dr R. Levin's assistance is gratefully acknowledged. So are the useful discussions with Dr D. Elata and Dr I. Bucher.

REFERENCES

Aoki, S. and Kimura, T. (1993) Finite element study of the optical method of caustic for measuring impact fracture toughness. *Journal of the Mechanics and Physics of Solids* **41**(3), 413–425.

ANSYS, User's Manual (1994) Swanson Analysis Systems Inc.

Boley, B. A. and Weiner, J. H. (1960) *Theory of Thermal Stresses*. John Wiley and Sons, New York, NY.

Bendersky, D. (1953) A special thermocouple for measuring transient temperatures. *Mechanical Engng*, February 1953, 117–121.

Bui, H. D., Maigre, H. and Rittel, D. (1992) A new approach to the experimental determination of the dynamic stress intensity factor. *International Journal of Solids Structures* **29**(23), 2881–2895.

Carslaw, H. S. and Jaeger, J. C. (1959) *Conduction of Heat in Solids*. Oxford University Press, Oxford, U.K.

Chou, S. C., Robertson, K. D. and Rainey, J. H. (1973) The effect of strain rate and heat developed during deformation on the stress–strain curve of plastics. *Experimental Mechanics*, October 1973, 422–432.

Döll, W. (1976) Application of an energy balance and an energy method to dynamic crack propagation. *International Journal of Fracture* **12**(4), 595–605.

Freund, L. B. and Rosakis, A. J. (1992) The structure of the near-tip field during transient elastodynamic crack growth. *Journal of the Mechanics and Physics of Solids* **40**(3), 699–719.

Fuller, K. N. G., Fox, P. G. and Field, J. E. (1975) The temperature rise at the tip of a fast-moving crack in glassy polymers. *Proceedings of the Royal Society* **A341,** 537–557.

Kalthoff, J. F. and Shockey, D. A. (1977) Instability of cracks under impulse loads. *Journal of Applied Physics* **48,** 986–993.

Lifshitz, J. M. and Leber, H. (1994) Data processing in the split Hopkinson pressure bar tests. *Int. J. Impact Engng* **15**(6), 723–733.

Maigre, H. and Rittel, D. (1993) Mixed-mode quantification for dynamic fracture initiation: application to the compact compression specimen. *International Journal of Solids and Structures* **30**(23), 3233–3244.

Maigre, H. and Rittel, D. (1996) Dynamic fracture detection using the force-displacement reciprocity: application to the compact compression specimen. *International Journal of Fracture* **73**(1), 67–79.

Meyers, M. A. (1994) *Dynamic Behavior of Materials*. John Wiley and Sons, New York, NY.

Rittel, D. (1997) *Thermoelastic Effects in Dynamic Fracture*, Technion Report, TME 453.

Rittel, D., Levin, R. and Maigre, H. (1997) On dynamic crack initiation in polycarbonate under mixed-mode loading. *Mechanics Research Communications* **24**(1), 57–64.

Rittel, D. and Maigre, H. (1996) An investigation of dynamic crack initiation in PMMA. *Mechanics of Materials* **23,** 229–239.

Rittel, D., Maigre, H. and Bui, H. D. (1992) A new method for dynamic fracture toughness testing. *Scripta Metallurgica et Materialia* **26,** 1593–1598.

Taylor, G. I. and Quinney, H. (1934) The latent energy remaining in a metal after cold working. *Proceedings of the Royal Society* **A143,** 307–326.

Weichert, R. and Schönert, K. (1978) Heat generation at the tip of a moving crack. *Journal of the Mechanics and Physics of Solids* **26,** 151–161.

Zehnder, A. T. and Rosakis, A. J. (1991) On the temperature distribution at the vicinity of dynamically propagating cracks in 4340 steel. *Journal of the Mechanics and Physics of Solids* **39**(3), 385–415.

Zhou, M., Rosakis, A. J. and Ravichandran, G. (1996) Dynamically propagating shear bands in impact-loaded prenotched plates. I—Experimental investigations of temperature signatures and propagation speed. *Journal of the Mechanics and Physics of Solids* **44**(6), 981–1006.